

The mechanism by which nonlinearity sustains turbulence in plane Couette flow

M-A. Nikolaidis¹, B. F. Farrell², P. J. Ioannou¹

¹National and Kapodistrian University of Athens, Department of Physics, Panepistimiopolis, Zografos, 15784 Athens, Greece

²Department of Earth and Planetary Sciences, Harvard University, Cambridge, MA 02138, USA

E-mail: pjioannou@phys.uoa.gr

Abstract. Turbulence in wall-bounded shear flow results from a synergistic interaction between linear non-normality, by which a subset of perturbations configured to transfer energy from the mean component of the turbulent state to the perturbation component maintain the perturbation field energy, and nonlinearity by which the subset of energy-transferring perturbations is replenished and maintained in the statistically steady state. Although it is accepted that both linear non-normality mediated energy transfer and nonlinear interactions among perturbations are required to maintain the turbulent state, the detailed physical mechanism by which these processes operate to maintain the turbulent state has not been determined. In this work a statistical state dynamics based analysis is performed demonstrating that the perturbation component in Couette flow turbulence is maintained by a parametric growth process associated with marginal Lyapunov stability of the streamwise mean flow, and that interaction among streamwise varying components of the perturbation field does not contribute positively to the maintenance of the turbulent state. This work identifies the parametric interaction between the fluctuating streamwise mean and the streamwise varying perturbations to be the mechanism of the nonlinear interaction maintaining the turbulent state, and identifies the associated Lyapunov vectors with positive energetics as the energetically active perturbation subspace.

1. Introduction

Turbulence is widely regarded as the primary exemplar of an essentially nonlinear phenomenon. However, the mechanism by which energy is transferred in shear flows from the externally forced component of the flow to the broad spectrum of spatially and temporally varying perturbations is through linear non-normal interaction between these flow components [1, 2]. Nevertheless, nonlinearity participates in an essential way in this cooperative interaction by which turbulence self-sustains. Our goal in this study is to provide a more comprehensive understanding of the role of nonlinearity and its interaction with linear non-normality in the maintenance of turbulence.

In order to study the mechanism by which nonlinearity between streamwise varying components participates in the maintenance of turbulence in shear flow we begin by partitioning the velocity field of plane parallel Couette flow into streamwise mean and perturbation components, or equivalently into the $k_x = 0$ and the $k_x \neq 0$ components of the Fourier decomposition of the flow field, where k_x is the wavenumber in the streamwise, x , direction. In this decomposition the flow field is partitioned as:

$$\mathbf{u} = \mathbf{U}(y, z, t) + \mathbf{u}'(x, y, z, t), \quad (1)$$

with cross-stream direction y and spanwise direction z . Note that in this decomposition the mean flow retains temporal variation in its spanwise structure as would occur e.g. in the presence of time-dependent streaks.

The non-dimensional Navier-Stokes equations expressed using this mean and perturbation partition are:

$$\partial_t \mathbf{U} + \underbrace{\mathbf{U} \cdot \nabla \mathbf{U}}_{N_1} + \nabla P - \Delta \mathbf{U} / R = - \underbrace{\langle \mathbf{u}' \cdot \nabla \mathbf{u}' \rangle_x}_{N_2}, \quad (2a)$$

$$\partial_t \mathbf{u}' + \underbrace{\mathbf{U} \cdot \nabla \mathbf{u}' + \mathbf{u}' \cdot \nabla \mathbf{U}}_{N_3} + \nabla p' - \Delta \mathbf{u}' / R = - \underbrace{(\mathbf{u}' \cdot \nabla \mathbf{u}' - \langle \mathbf{u}' \cdot \nabla \mathbf{u}' \rangle_x)}_{N_4}, \quad (2b)$$

$$\nabla \cdot \mathbf{U} = 0, \quad \nabla \cdot \mathbf{u}' = 0, \quad (2c)$$

where $R = U_w h / \nu$ is the Reynolds number and $\pm U_w$ the wall velocity at $y = \pm h$. The flow satisfies no-slip boundary conditions in the cross-stream direction: $\mathbf{U}(x, \pm h, z, t) = (\pm U_w, 0, 0)$, $\mathbf{u}'(x, \pm h, z, t) = (0, 0, 0)$ and periodic boundary conditions in the z and x directions. Averaging is denoted with a bracket $\langle \cdot \rangle$ with the bracket subscript indicating the averaging variable, so that e.g. the streamwise mean velocity is $\mathbf{U} \equiv \langle \mathbf{u} \rangle_x = L_x^{-1} \int_0^{L_x} \mathbf{u} dx$, where L_x is the streamwise length of the channel. The Navier-Stokes equations with this decomposition will be referred to as the NL system. We have indicated with an underbrace the non-linear terms in the NL system. The advective term in (2a) with the nonlinear interactions between $k_x = 0$ flow components will be referred to as N_1 , the Reynolds stress divergence term in (2a), produced by nonlinear interaction between the k_x and $-k_x$ flow components with $k_x \neq 0$, will be referred to as N_2 . In (2b) N_3 gives the nonlinear interaction between the mean flow and the $k_x \neq 0$ flow components, which is also the source of the non-normality of the operator governing the perturbation evolution, and N_4 is the eddy-eddy nonlinear interactions between $k_{x1} \neq 0$ and $k_{x2} \neq 0$, with $k_{x1} \neq -k_{x2}$.

Transition to and maintenance of a self-sustained turbulent state results even when only nonlinearities N_1, N_2 and N_3 are retained [3]. By retaining N_3 in addition to nonlinearities N_1 and N_2 we obtain the restricted non-linear system (RNL):

$$\partial_t \mathbf{U} + \mathbf{U} \cdot \nabla \mathbf{U} + \nabla P - \Delta \mathbf{U} / R = - \langle \mathbf{u}' \cdot \nabla \mathbf{u}' \rangle_x, \quad (3a)$$

$$\partial_t \mathbf{u}' + \mathbf{U} \cdot \nabla \mathbf{u}' + \mathbf{u}' \cdot \nabla \mathbf{U} + \nabla p' - \Delta \mathbf{u}' / R = 0, \quad (3b)$$

$$\nabla \cdot \mathbf{U} = 0, \quad \nabla \cdot \mathbf{u}' = 0. \quad (3c)$$

It has been confirmed that this RNL system supports a realistic self-sustaining process (SSP) which maintains a turbulent state in minimal channels [3, 4], in channels of moderate sizes at both low and high Reynolds numbers (at least for $R_\tau \leq 1000$) [5–7], and also in very long channels [8].

Consider in isolation the time varying mean flow \mathbf{U} obtained from a state of turbulence either of the NL equations or of the RNL system. Small perturbations, \mathbf{u}' , on this mean flow evolve in the linear approximation according to

$$\partial_t \mathbf{u}' + \mathbf{U} \cdot \nabla \mathbf{u}' + \mathbf{u}' \cdot \nabla \mathbf{U} + \nabla p' - \Delta \mathbf{u}' / R = 0, \quad \nabla \cdot \mathbf{u}' = 0, \quad (4)$$

which is exactly the perturbation equation (3b) of the RNL system, while in the NL system the actual \mathbf{u}' obeys the different equation (2b) with the N_4 term included. In the self-sustained RNL turbulent state the perturbation flow velocity, \mathbf{u}' , that evolves under (3b) or equivalently under (4) remains finite and bounded. Therefore the mean-flow, \mathbf{U} , of the RNL turbulent state is stable in the sense that perturbations, i.e. the streamwise varying flow components, \mathbf{u}' , that evolve under (4), remain bounded and therefore have zero asymptotic growth rate and the mean flow can be considered to be in the critical state of neutrality, poised between stability and instability.

The question that will be addressed in this paper is whether the mean flow, \mathbf{U} , that obtains in NL turbulence is similarly neutral in the sense that perturbations, \mathbf{u}' , that evolve under (4), remain bounded and therefore have vanishing asymptotic growth rate and the mean flow can be also be considered to be in the critical state of neutrality. If the turbulent mean flow \mathbf{U} of NL is neutral, in the sense discussed above, then the mean flow structure is controlled through quasi-linear interaction with the perturbation field and the turbulent dynamics are in essence RNL dynamics.

The above are related to a conjecture of Malkus [9]. Malkus conjectured that the state of anisotropic turbulence is such that: “First, that the mean flow will be statistically stable if an Orr-Sommerfeld type equation is satisfied by fluctuations of the mean; second, that the smallest scale of motion that can be present in the spectrum of the momentum transport is the scale of the marginally stable fluctuations of the mean”. Thus, Malkus conjectures that the turbulent mean state is brought into a state of neutrality. While e.g. turbulent convection [10, 11] and the baroclinic turbulence in the midlatitude atmosphere [12] display a usefully close approximate adherence to this conjecture, the turbulent mean state of wall-bounded turbulence, defined as the streamwise, spanwise and temporal mean, $\langle \mathbf{U} \rangle_{z,t}$, is hydrodynamically stable and far from neutrality in apparently strong violation of the Malkus conjecture if the mean is interpreted to be the streamwise, spanwise and temporal mean [13]. However, RNL turbulence suggests that the program of Malkus [9] to wall turbulence was essentially correct requiring only the additional recognition that the instability to be equilibrated is the instability of the time-dependent operator associated with linearization about the temporally varying streamwise mean flow, \mathbf{U} . The growth rate of the fluctuations to the mean \mathbf{U} that are governed by (4) is given by the maximal Lyapunov exponent of \mathbf{u}' given by

$$\lambda_{Lyap} = \lim_{t \rightarrow \infty} \frac{\log |\mathbf{u}'|}{t}, \quad (5)$$

and RNL turbulence with the definition of mean of (1) satisfies the Malkus conjecture precisely and

$$\lambda_{Lyap} = 0. \quad (6)$$

RNL turbulence satisfies the Malkus conjecture as interpreted above. The question that will be discussed in this paper is whether NL turbulence (with the N4 term included) is similarly neutral in the Lyapunov sense. By that we mean whether fluctuations, \mathbf{u}' , evolving under (4) on the time dependent mean flow, \mathbf{U} , that obtains in a turbulent simulation of the NL equations, have λ_{Lyap} , as defined in (6), approximately zero. We caution the reader to observe that the Lyapunov exponents we are calculating are not the Lyapunov exponents of perturbations on the turbulent trajectory, which is associated with the growth of perturbations $\delta \mathbf{U}$, $\delta \mathbf{u}'$ under the linearized dynamics of the full NL system about the turbulent trajectory \mathbf{U} , \mathbf{u}' . The turbulent trajectory is chaotic and will have many of these Lyapunov exponents positive, while perturbations tangent to the trajectory will have zero Lyapunov exponent. We instead assume \mathbf{U} to be the mean flow that obtains in a simulation and calculate the Lyapunov exponent of perturbations, \mathbf{u}' , evolving under the linear dynamics (4) about this given time dependent mean flow \mathbf{U} .

It could be argued that the choice of the mean on which the asymptotic growth rate of perturbations is predicated is arbitrary. However, statistical state dynamics (SSD) analysis reveals that transition to and maintenance of turbulence occurs in association with the breaking of statistical symmetries of the laminar state through a sequence of bifurcations. The laminar state in Couette flow has spanwise, streamwise and temporal statistical homogeneity. When the SSD of Couette flow is closed at second order it has been shown that at a first critical Reynolds number the spanwise symmetry is broken, and at a second higher Reynolds number the temporal statistical homogeneity is also broken, coincident with transition to the turbulent state [3, 4]. Given that in this SSD turbulent state the spanwise and temporal homogeneity has been broken, we propose that it is inappropriate and dynamically inconsistent to use either the spanwise or the

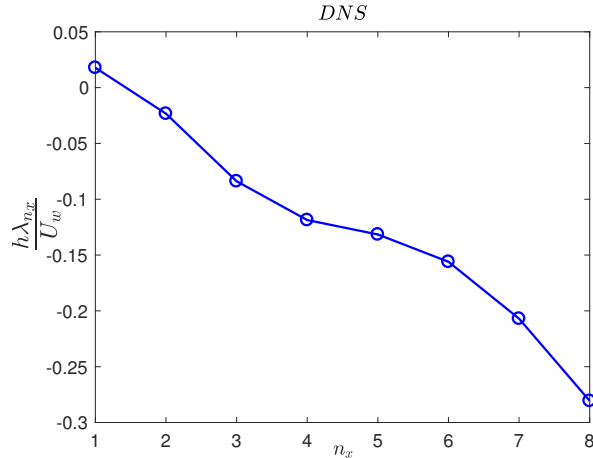


Figure 1. The top Lyapunov exponent of perturbations with channel wavenumbers $n_x = 1, \dots, 8$ evolving under the time-dependent NL turbulent flow, \mathbf{U} . The Lyapunov exponent of \mathbf{u}' of all $n_x \geq 2$ components is negative. We non-dimensionalize the Lyapunov exponent and any growth rate mentioned in the text using advective time units, h/U_w . For comparison, the least stable mode of the streamwise-spanwise-temporal mean of \mathbf{U} has growth rate $\sigma = -0.12$ that occurs at $n_x = 1$ and spanwise wavenumber $k_z = 6\pi/L_z$. A plane Couette channel at $R = 600$ was used.

temporal mean to partition the flow field into mean and perturbation components. It is necessary for dynamic consistency to allow both spanwise and temporal variations in structure requiring representation (1) in order to analyze the turbulent state. It remains an open question whether in the turbulent state the streamwise statistical homogeneity is also broken. The evidence that is usually presented to support breaking of the streamwise statistical homogeneity is that no arbitrarily long streamwise structures are observed in simulations, but this evidence is based on individual realizations which may not reflect the symmetries of the statistical state. The evidence supporting the non-breaking of the streamwise symmetry is that RNL turbulence has been shown to support a turbulent state with the assumption of a streamwise mean ($k_x = 0$) in long turbulent channels, demonstrating that there exists a statistical turbulent state with statistical streamwise homogeneity [8].

RNL turbulence satisfies the Malkus conjecture as discussed above and the question to be addressed is whether NL turbulence produces a similarly neutral mean flow, \mathbf{U} . Comparing RNL and NL dynamics provides a new perspective on the analysis of the role of the perturbation-perturbation nonlinearity N4 in the maintenance and regulation of turbulence in wall-bounded shear flows. The N4 term in (2b), denoted as \mathbf{f} , does not contribute directly to maintaining the perturbation energy because the perturbation-perturbation interactions redistribute energy internally among the streamwise $k_x \neq 0$ components of the flow and the term $\langle \mathbf{u}' \cdot \mathbf{f} \rangle_{x,y,z}$ is zero¹. Consequently, from (2b) we obtain that the perturbation energy density, $E_p = \langle |\mathbf{u}'|^2/2 \rangle_{x,y,z}$, evolves according to:

$$\frac{dE_p}{dt} = \underbrace{\langle \mathbf{u}' \cdot (-\mathbf{U} \cdot \nabla \mathbf{u}' - \mathbf{u}' \cdot \nabla \mathbf{U} + \Delta \mathbf{u}'/R) \rangle_{x,y,z}}_{\dot{E}_{linear}}. \quad (7)$$

just as in RNL turbulence. The term \dot{E}_{linear} , in the underbrace, indicates the energy transferred to the streamwise-varying perturbations by what is considered to be the linear interaction with

¹ In our simulations time discretization produces a $\langle \mathbf{u}' \cdot \mathbf{f} \rangle_{x,y,z,t}$ of the order of $-0.0005U_w^3/h$ and sets an error-bar for the accuracy of our results.

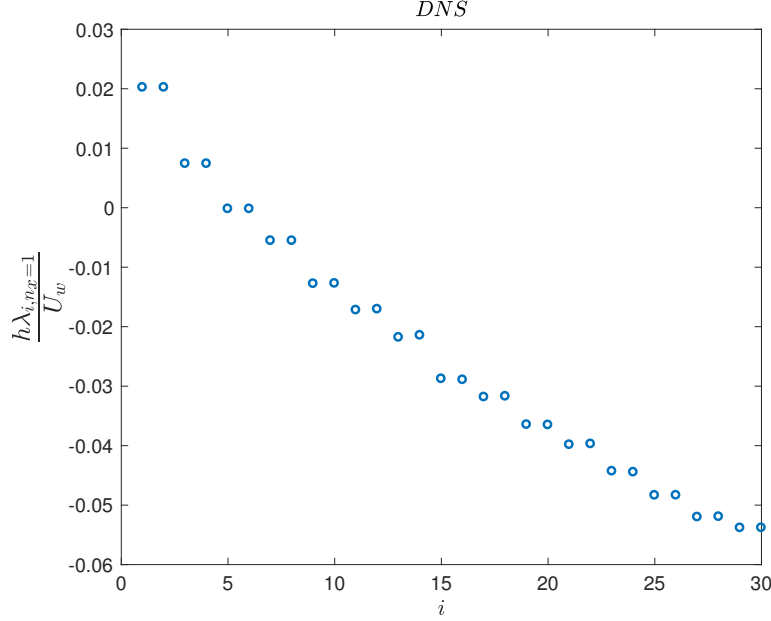


Figure 2. The largest 30 Lyapunov exponents of $n_x = 1$ perturbations to the NL turbulent flow, \mathbf{U} . Note that each exponent corresponds to two states that allow for streamwise translation of the Lyapunov vector.

the mean \mathbf{U} . The Lyapunov exponent of the \mathbf{u}' that evolves under (4) with the mean flow, \mathbf{U} , from the NL simulation can be equivalently obtained as the time-average of the instantaneous energy growth rates:

$$\lambda_{Lyap} = \left\langle \frac{1}{2E_p} \frac{dE_p}{dt} \right\rangle_t . \quad (8)$$

Equation (8) gives the maximum Lyapunov exponent (MLE) of the perturbation dynamics, but a full spectrum of exponents can also be obtained through orthogonalization techniques [14]. This exponent should be contrasted to the similar exponent that is obtained if \mathbf{u}' is taken to be actually the perturbation flow associated with the \mathbf{U} of the NL turbulent state. This \mathbf{u}' is bounded and produces zero effective growth rate in a NL simulation and therefore:

$$\lambda_{state} = \left\langle \frac{\langle \mathbf{u}' \cdot (-\mathbf{U} \cdot \nabla \mathbf{u}' - \mathbf{u}' \cdot \nabla \mathbf{U} + \Delta \mathbf{u}' / R) \rangle_{x,y,z}}{2E_p} \right\rangle_t = 0. \quad (9)$$

It will illuminate the analysis to compare the rate of energy transfer to the perturbations from the mean flow:

$$\dot{E}_{def} = \langle \mathbf{u}' \cdot (-\mathbf{U} \cdot \nabla \mathbf{u}' - \mathbf{u}' \cdot \nabla \mathbf{U}) \rangle_{x,y,z} , \quad (10)$$

for the actual \mathbf{u}' from the NL simulation to the rate of energy transfer when \mathbf{u}' evolves linearly under (4). Similarly we can compare the perturbation energy dissipation rates:

$$\dot{E}_{dissip} = \frac{1}{R} \langle \mathbf{u}' \cdot \Delta \mathbf{u}' \rangle_{x,y,z} . \quad (11)$$

We note that the Lyapunov exponent (8) or the effective growth rate of the perturbations (9) evolving on mean flow \mathbf{U} can be obtained from the sum of these terms

$$\left\langle \frac{\dot{E}_{def} + \dot{E}_{dissip}}{2E_p} \right\rangle_t . \quad (12)$$

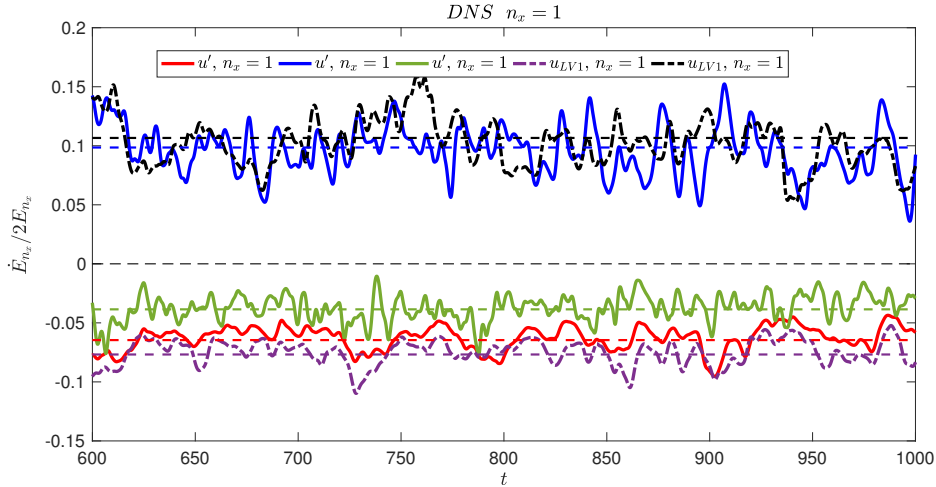


Figure 3. Contribution to the instantaneous energy growth rate of the $n_x = 1$ perturbation component of the NL simulation: extraction from the fluctuating $n_x = 0$ mean component $\dot{E}_{def,n_x}/(2E_{n_x})$ (blue, solid); the rate of energy loss to dissipation $\dot{E}_{dissip,n_x}/(2E_{n_x})$ (red, solid); and the rate of transfer to the other $n_x > 1$ streamwise components (green, dotted). The mean values of these rates are indicated with the dashed lines with the corresponding color and arrows. These average rates sum to $\lambda_{state} = 0$. The corresponding rates for the first Lyapunov vector on the same fluctuating $n_x = 0$ mean flow, which is also a $n_x = 1$ flow component, are shown in black and purple dash-dotted lines (there is no energy transfer to the other components as N4 is absent in this calculation). These rates sum to the Lyapunov exponent $\lambda_{Lyap} = 0.02U_w/h$. This figure shows that the nonlinear interactions perturbation - perturbation nonlinearity, N4, disrupts the parametric energetic interaction of the perturbations with the mean rather than configuring the perturbations so as to extract more energy from the mean flow.

The dynamical significance of N4 in sustaining the turbulent state is revealed by comparing the perturbation energetics of the NL mean flow \mathbf{U} with and without the term N4. This can be achieved by calculating λ_{Lyap} of the \mathbf{U} obtained from NL together with the associated contributions to this growth rate from \dot{E}_{def} and \dot{E}_{dissip} and comparing these rates to those obtained when the term N4 is included. Although the N4 term is energetically neutral it may have a profound impact on the energetics by modifying the perturbations to extract more or less energy from the mean flow. If the term N4 is not fundamental to sustaining turbulence, the λ_{Lyap} computed with \mathbf{U} of the NL turbulence would be zero or close to zero as in RNL, strongly suggesting that the interaction between mean and perturbations is the central dynamical interaction and that the turbulence is supported primarily through the parametric perturbation growth process associated with the temporal variation of \mathbf{U} , without substantial contribution from the N4 nonlinearity. The alternative is that the N4 term has a first-order effect on the energetics which implies centrality in the dynamics of turbulence of the alternative role for N4 which is replenishing the subset of perturbations lying in the directions of growth as in many toy models of turbulence dynamics [15–18]. This distinction in mechanism can be clarified by observing that, if the mean flow is chosen to be the streamwise-spanwise-temporal mean, which in a boundary layer flow is the stable Reynolds-Tiederman profile [13], the N4 nonlinearity must assume this role in sustaining the turbulent state and statistically stationary self-sustained turbulence is only possible if the N4 term is sufficiently effective in scattering perturbations back into the directions of non-normal growth. However, it is known that turbulence is not sustained with this choice of mean flow [19].

Table 1. The channel is periodic in the streamwise, x , and spanwise, z , direction and at the channel walls $y = \pm h$ the velocity is $\mathbf{u} = (\pm U_w, 0, 0)$. The channel length is L_x and L_z in the streamwise and spanwise directions respectively. The number of streamwise and spanwise Fourier components is N_x and N_z after dealiasing in the streamwise and spanwise direction by the 2/3 rule, and we use N_y grid points in the wall-normal direction. $R = U_w h / \nu$ is the Reynolds number of the simulation, with ν the kinematic viscosity.

Parameter	$[L_x, L_z]/h$	$N_x \times N_z \times N_y$	R
NS600	$[1.75\pi, 1.2\pi]$	$17 \times 17 \times 35$	600

2. The Lyapunov exponent of the mean flow in Couette turbulence at $R = 600$

Consider a Couette turbulence simulation at $R = 600$ in a periodic channel with parameters given in Table 1. This is a larger channel compared to the minimal Couette flow that was studied by Hamilton, Kim & Waleffe [20] at $R = 400$. RNL turbulence with these parameters at $R = 600$ was systematically examined recently [21].

We first calculate the Lyapunov exponent λ_{Lyap} of the NL mean flow by estimating (8) from a long integration of (4) with the mean flow \mathbf{U} obtained from a turbulent NL simulation. The initial state \mathbf{u}' is inconsequential because with measure zero exception any random initial condition converges with exponential accuracy to the structure associated with the largest Lyapunov exponent. The full spectrum of Lyapunov exponents can be obtained by an orthogonalization procedure with the inner product of two flow fields, \mathbf{u}'_1 and \mathbf{u}'_2 , defined as the volume integral of the dot product of the velocities: $\langle \mathbf{u}'_1 \cdot \mathbf{u}'_2 \rangle_{x,y,z}$. For a discussion of the calculation and the properties of Lyapunov exponents and the structures associated with them refer to Refs. [14, 21–24]. Because of the streamwise independence of \mathbf{U} the different streamwise Fourier components of \mathbf{u}' in this Lyapunov exponent calculation, in which the N4 term is absent, evolve independently and the structure (the Lyapunov vector) associated with a given Lyapunov exponent has streamwise structure confined to a single streamwise wavenumber $k_x = 2\pi n_x h / L_x$ corresponding to channel streamwise wavenumber n_x . The largest Lyapunov exponent at each n_x is shown in Fig. 1. This figure reveals that the time dependent streamwise mean flow component \mathbf{U} is nearly neutral with only the $n_x = 1$ streamwise component supporting a small positive Lyapunov exponent $\lambda_{Lyap} \approx 0.02U_w/h$. For comparison the least stable mode of the streamwise-spanwise-temporal mean flow, $\langle \mathbf{U} \rangle_{x,z,t}$, in this channel has growth rate $\sigma = -0.12U_w/h$. Strictly speaking, the $n_x = 1$ component is associated with a pair of Lyapunov exponents corresponding to the real and imaginary part of a single structure. This degeneracy of the Lyapunov exponents results from the streamwise homogeneity of the linear operator which implies that the streamwise phase of the Lyapunov vectors is arbitrary. The growth rates of the first 30 Lyapunov exponents associated with $n_x = 1$ ordered descending in their growth rate are shown in Fig. 2. Specifically, the perturbation subspace is spanned by a set of Lyapunov vectors comprised of a pair of structures sharing a single spanwise/cross-stream structure but having respectively $\sin(k_x x)$ and $\cos(k_x x)$ streamwise dependence. From Fig. 2 it is apparent that at this Reynolds number and for this minimal channel the NL turbulent mean flow supports only two small positive Lyapunov exponent pairs.

Contributions to the Lyapunov exponent from mean flow energy transfer and from dissipation are plotted as a function of time in Fig. 3. The growth rate associated with energy transfer from the fluctuating streamwise mean is on average $0.1066U_w/h$, while the dissipation rate is on average $0.0862U_w/h$ resulting in the slightly positive Lyapunov exponent $\lambda_{Lyap} = 0.0204U_w/h$. These transfers occur when perturbations evolve under the dynamics of the fluctuating streamwise

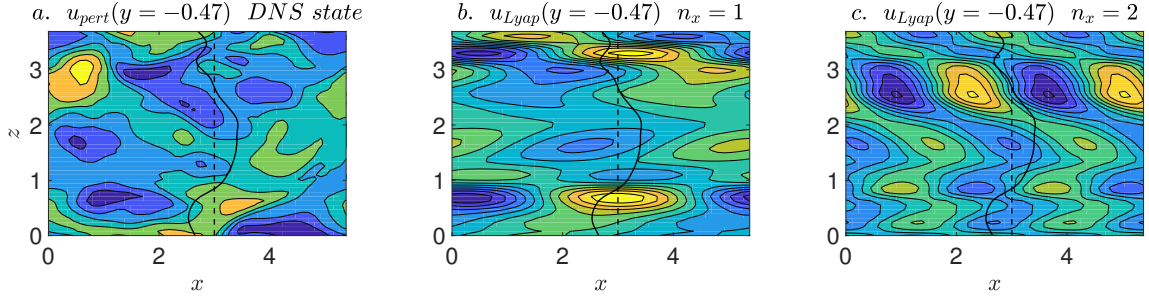


Figure 4. Snapshots at the same time showing the streamwise perturbation velocity u' of the NL state (panel (a)), of the top Lyapunov vector which has streamwise channel wavenumber $n_x = 1$ (panel (b)) and the decaying top Lyapunov vector associated with $n_x = 2$ (panel (c)). Also shown is the streak component of the streamwise mean flow $U - \langle U \rangle_z$ (black line).

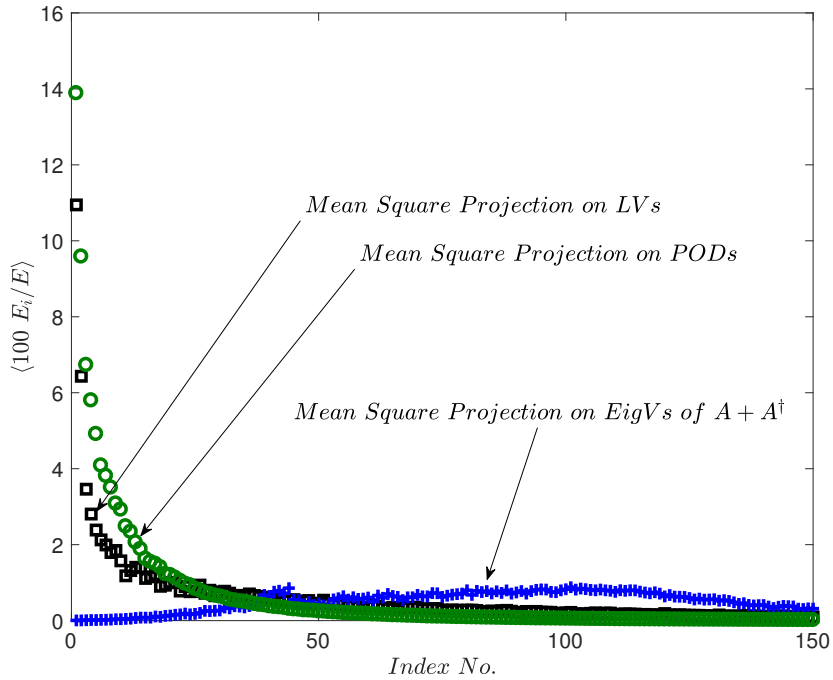


Figure 5. Average energy percentage of the $n_x = 1$ flow accounted for by each pair of Lyapunov vectors (black squares). Average energy percentage of the $n_x = 1$ flow accounted for by the eigenvectors of $A + A^\dagger$ ordered in descending order of their eigenvalue (blue crosses). A is the linear operator in (4) governing the linear evolution of the perturbations about \mathbf{U} , ordered in descending order of their eigenvalue. The eigenvectors of $A + A^\dagger$ are the orthogonal directions of stationary instantaneous perturbation energy growth rate, with this stationary growth rate given by the corresponding eigenvalue. The perturbation component of the turbulent flow is adjusted so as to have a small projection on the first eigenvectors of $A + A^\dagger$ associated with large instantaneous energy growth rates. Also shown is the energy percentage accounted for by the PODs of the $n_x = 1$ component of the NL perturbation state (green circles).

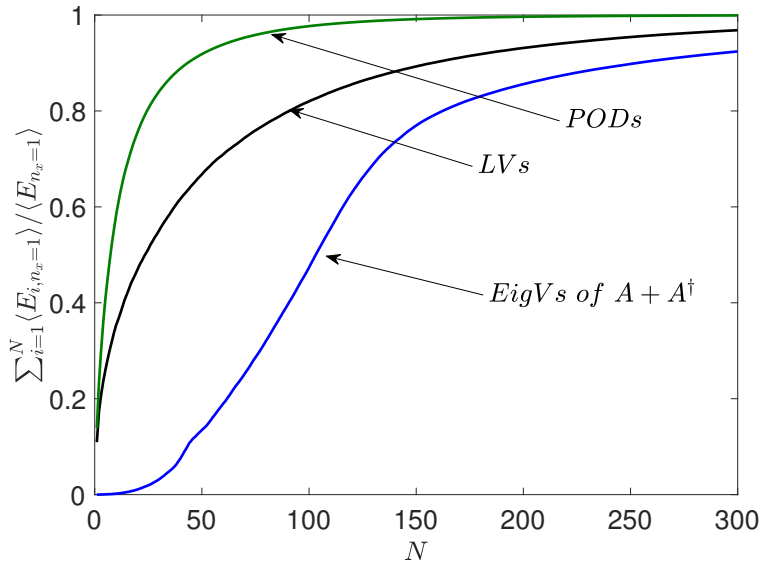


Figure 6. Average fraction of the energy of the $n_x = 1$ flow accounted for by the first N pairs of Lyapunov vectors (black), by the first N eigenvectors of $A + A^\dagger$ (blue) ordered in descending order of their eigenvalue, and by the first N POD's of the $n_x = 1$ component of the NL state (green).

mean flow \mathbf{U} associated with NL turbulence but in the absence of disturbance to the perturbation structure by the perturbation-perturbation nonlinearity N4 and they show that the mean flow has been adjusted close to neutral Lyapunov stability. Note that these time scales are comparable to the turbulent energy time scale defined as the ratio of the time rate of energy input from the walls to the kinetic energy of the flow, which is about $0.04U_w/h$.

We now contrast the energetics of the Lyapunov vectors on the turbulent NL mean flow just shown with the corresponding energetics of the $n_x = 1$ Fourier component of the state vector obtained from the turbulent NL simulation itself in order to determine whether the N4 term corresponding to perturbation-perturbation nonlinearity has the effect of influencing the perturbations to be in a more or less favorable configuration for extracting energy from the mean flow. These results are also shown in Fig. 3 from which it can be seen that the transfer from the mean \mathbf{U} with the influence of the N4 term included is slightly less than that achieved by the first Lyapunov vector in the absence of the influence of N4: the transfer to the NL state produces growth rate $0.0985U_w/h$ compared to $0.1066U_w/h$ for the case of the unperturbed Lyapunov vector on the NL mean flow. This demonstrates that the nonlinear term does not configure the flow states so as to extract more energy from the mean. However, despite the fact that the energy extracted from the mean flow by the NL perturbation state and the first Lyapunov vector are nearly equal when averaged over time, the correlation coefficient of their time series is low (0.26) indicating that the N4 term has disrupted the first Lyapunov vector and spread its energy to other Lyapunov vectors. The fact that this disruption does not substantially alter the time-mean energy extraction from the streamwise mean flow suggests that the time mean energetics resulting from projection on the Lyapunov vectors of \mathbf{U} is not substantially altered by N4 while the projection at an instant in time is (this projection is onto the single top Lyapunov vector when N4 is absent). To investigate this possibility we need to project the energetics on the Lyapunov vectors rather than on the growth directions associated with the eigenvectors of $A + A^\dagger$, with A the linear operator in (4) governing the linear evolution of the perturbations about \mathbf{U} . Note also that the decay rate of the NL flow state due to dissipation is

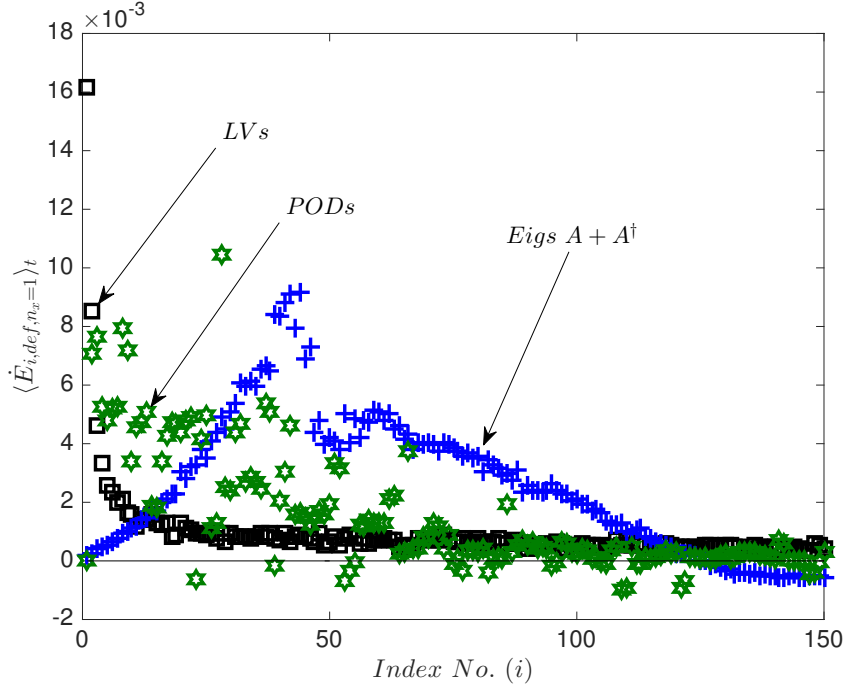


Figure 7. Contribution of the Lyapunov vectors (black squares), the PODs (green stars) and the eigenvectors of $A + A^\dagger$ (blue crosses) to the energy extraction rate, \dot{E}_{def} , from the mean flow.

$0.0646U_w/hU_w/h$ which is less than the corresponding decay rate of the first Lyapunov vector. This difference in decay rate is explained by reference to Fig. 4, from which it is apparent that the $n_x = 1$ perturbation component of the NL state is of larger scale than the $n_x = 1$ Lyapunov vector. Also, consider that, in the energetics of the $n_x = 1$ perturbation component in NL there is a term not present in the corresponding Lyapunov vector: the energy interchanged with the remaining $n_x \neq 0$ components, which is also shown in Fig. 3. The $n_x = 1$ perturbation component of the NL state exports energy to the other streamwise components of the flow and this nonlinear transfer contributes $0.0386U_w/h$ at this wavenumber to the decay rate. This additional decay, which corresponds to the eddy-viscosity at this scale, is just sufficient to reduce the mean growth rate of the NL state to the expected value $\lambda_{state} = 0$.

We conclude that the Lyapunov exponent of the fluctuating streamwise mean flow \mathbf{U} in NL turbulence has been adjusted to near neutrality which is consistent with its parametric growth process fully accounting for the maintenance of the perturbation component of the turbulent state. The perturbation-perturbation nonlinearity, N4, does not configure the perturbations to extract more energy from the mean flow than they would in the absence of this term implying that N4 acts as a disruption to the parametric growth process supporting the Lyapunov vector rather than augmenting the perturbation maintenance by the frequently hypothesized mechanism in which perturbation-perturbation nonlinearity replenishes the subspace of perturbations configured to transfer energy from the mean flow to the perturbations in order to maintain the turbulent state. The fact that the mean NL flow has been adjusted to near neutrality indicates that the first Lyapunov vector should be a dominant component of the NL perturbation state. This will be examined in the next section.

3. Analysis of perturbation energetics by projection onto the Lyapunov vector basis

Despite the persuasive correspondence between the mean energetics of the NL perturbation state and the mean energetics of the top Lyapunov vector calculated using the associated fluctuating streamwise mean flow, \mathbf{U} , snapshots of the perturbation state and the Lyapunov vectors shown in Fig. 4 reveal considerable differences between their velocity fields. This suggests further analysis to clarify the relation between the perturbation state and the Lyapunov vectors. The orthogonality property imposed on the Lyapunov vectors makes them an attractive basis for decomposition of the $n_x = 1$ component of the NL perturbation state for the purpose of analyzing the relation between perturbation structure and energetics. Expanding the Fourier amplitude of the $n_x = 1$ NL perturbation state $\hat{\mathbf{u}}'$ in the basis of the orthonormal in energy $n_x = 1$ Lyapunov vectors:

$$\hat{\mathbf{u}}'(t) = \sum_i a_i(t) \mathbf{u}_{LV_i}(t), \quad (13)$$

with projection coefficient:

$$a_i(t) = \langle \mathbf{u}_{LV_i}(t) \cdot \hat{\mathbf{u}}'(t) \rangle_{x,y,z}, \quad (14)$$

we obtain that the contribution to the energy of the perturbations accounted for by projection of the perturbation state on Lyapunov vector u_{LV_i} is $E_i = a_i^2(t)/2$. The projection of the energy of the $n_x = 1$ component of the perturbation state on the first 15 Lyapunov vectors is shown in Fig. 5. The percentage of energy accounted for by projection on the most unstable Lyapunov vector is 11%, significantly larger than the energy in each of the remaining Lyapunov vectors. Adding the second unstable Lyapunov vector raises this value to 17.4% and the first 100 $n_x = 1$ Lyapunov vectors account for 82% of the energy of the $n_x = 1$ component of the perturbation state as seen in Fig. 6. In order to understand the significance of the Lyapunov vectors as a basis for representing the NL perturbation state we have determined the orthonormal structures of the proper orthogonal decomposition (PODs) of the $n_x = 1$ component of the NL flow with the methods discussed in [25]. Fig. 5 and Fig. 6 demonstrates that the Lyapunov vectors provide a good representation of the NL perturbation state. We conclude that the energy of the perturbation state is partitioned into the Lyapunov vectors in the order of their Lyapunov exponent and that the Lyapunov vectors are a good basis to represent the perturbation turbulent state.

In Fig. 5 we also show the average projection of the NL state on the eigenvectors of the time-mean operator $A + A^\dagger$ ordered in descending order of its eigenvalue. A is the linear operator in (4) governing the linear evolution of the perturbations about \mathbf{U} . The eigenvectors of $A + A^\dagger$ are the orthogonal directions associated with instantaneous energy growth rate of perturbations on the flow, \mathbf{U} . The perturbation component has small projection on the first eigenvectors of $A + A^\dagger$ which are the structures producing greatest instantaneous energy growth rates. The turbulent mean flow \mathbf{U} is such that perturbations that lead to large instantaneous growth rate have large spanwise wavenumber and are located at the very high shear regions next to the channel boundaries. Consequently, the state has a small projection on the structures producing the most rapid instantaneous growth and the turbulent perturbation component is concentrated on the directions with small positive instantaneous growth rate. Small projection of the perturbation state on the directions of maximum instantaneous growth rate was also seen in RNL simulations at $R = 600$ [21].

In RNL simulations at $R = 600$ the perturbation turbulent state is entirely supported by the top Lyapunov vector and the energetics of the perturbation state consequently are the energetics of this single Lyapunov vector. The N4 nonlinearity distributes the perturbation energy over a subspace spanned primarily by the first few Lyapunov vectors, as shown in Fig. 5.

We can determine the distribution of the first N Lyapunov vectors ordered in contribution to the perturbation state energy growth rate, \dot{E}_{def} by calculating

$$\sum_{i=1}^N \dot{E}_{i,def} \equiv \langle \mathbf{u}'_N \cdot (-\mathbf{U} \cdot \nabla \mathbf{u}'_N - \mathbf{u}'_N \cdot \nabla \mathbf{U}) \rangle_{x,y,z,t}, \quad (15)$$

where

$$\mathbf{u}'_N(t) = \text{Re} \left(\sum_{i=1}^N a_i(t) \mathbf{u}_{LV_i}(t) e^{2\pi i x / L_x} \right), \quad (16)$$

is the truncation of the representation of the $n_x = 1$ perturbation state, given in (13), to the first N Lyapunov vectors. From that calculation, we can then obtain the incremental contribution, $E_{i,def}$, by each Lyapunov vector. We can similarly determine the contribution of each of the eigenvectors of $A + A^\dagger$ and of the PODs to the energetics of the perturbation state. The results, shown in Fig. 7, reveal that the Lyapunov vectors provide the primary support for the energetics and their energetic contribution follows the Lyapunov vector growth ordering.

4. Discussion

Statistical state dynamics based analysis of the transition to turbulence in Couette flow has revealed the sequence of symmetry breaking bifurcations of the statistical state of the flow as the Reynolds number increases [3, 4]. First the spanwise statistical symmetry of the laminar state is broken and when later the temporal statistical symmetry is broken transition to the turbulent state occurs. Second-order closure of the statistical state dynamics, has demonstrated that a realistic self-sustained turbulent state is maintained by interaction between the temporally and spanwise varying streamwise-mean flow and the associated perturbation component of the flow [5, 6, 8]. In these model systems the streamwise-mean flow is adjusted exactly to neutral stability, with the understanding that the time dependent streamwise mean flow is considered neutral when the first Lyapunov exponent is zero. This result allows a reinterpretation of the Malkus conjecture that the statistical state of inhomogeneous turbulence has mean flow that is adjusted to neutral hydrodynamic stability.

5. Conclusions

In this work the results for support of the perturbation variance and energetics obtained using statistical state dynamics in the RNL implementation were extended to DNS. The support of both the energy and energetics is on a single feedback neutralized Lyapunov vector in the case of RNL. In the case of DNS it was found that the energy and energetics are concentrated in the subspace spanned by the Lyapunov vectors and this support was ordered in the vectors according to their associated exponents with the top vector being marginally stable. The neutrality of the top Lyapunov vector in both RNL and DNS is interpreted as implying that the Malkus conjecture is valid and that consistently the perturbation structure is concentrated on the top Lyapunov vectors of the time varying streamwise-mean flow. The similarity of the dynamical support of RNL and DNS turbulence on the marginally stable Lyapunov structures with parametric growth mechanism vindicates the conjecture that the dynamically relevant mean flow in turbulent shear flow is not the streamwise-spanwise-temporal mean flow but rather the time and spanwise varying streamwise-mean flow which incorporates the statistical symmetries obtained from study of second order closures of the statistical state dynamics of wall-bounded turbulence.

Acknowledgments

This work was funded in part by the Coturb program of the European Research Council. We thank Javier Jimenez for his reviewing comments. Marios-Andreas Nikolaidis acknowledges the support of the Hellenic Foundation for Research and Innovation (HFRI) and the General Secretariat for Research and Technology (GSRT).

References

- [1] Henningson D S and Reddy S C 1994 On the role of linear mechanisms in transition to turbulence *Phys. Fluids* **6** 1396–1398
- [2] Kim J and Lim J 2000 A linear process in wall bounded turbulent shear flows *Phys. Fluids* **12** 1885–1888
- [3] Farrell B F and Ioannou P J 2012 Dynamics of streamwise rolls and streaks in turbulent wall-bounded shear flow *J. Fluid Mech.* **708** 149–196
- [4] Farrell B F, Ioannou P J and Nikolaidis M A 2017 Instability of the roll–streak structure induced by background turbulence in pretransitional Couette flow *Phys. Rev. Fluids* **2** 034607
- [5] Thomas V, Lieu B K, Jovanović M R, Farrell B F, Ioannou P J and Gayme D F 2014 Self-sustaining turbulence in a restricted nonlinear model of plane Couette flow *Phys. Fluids* **26** 105112
- [6] Farrell B F, Ioannou P J, Jiménez J, Constantinou N C, Lozano-Durán A and Nikolaidis M A 2016 A statistical state dynamics-based study of the structure and mechanism of large-scale motions in plane Poiseuille flow *J. Fluid Mech.* **809** 290–315
- [7] Farrell B F, Gayme D F and Ioannou P J 2017 A statistical state dynamics approach to wall-turbulence *Phil. Trans. R. Soc. A* **375** 20160081
- [8] Thomas V, Farrell B F, Ioannou P J and Gayme D F 2015 A minimal model of self-sustaining turbulence *Phys. Fluids* **27** 105104
- [9] Malkus W V R 1956 Outline of a theory of turbulent shear flow *J. Fluid Mech.* **1** 521–539
- [10] Malkus W V R 1954 The heat transport and spectrum of thermal turbulence *Proc. Roy. Soc. A.* **225** 196–212
- [11] Malkus W V R and Veronis G 1958 Finite amplitude cellular convection *J. Fluid Mech.* **4** 225–260
- [12] Stone P H 1978 Baroclinic adjustment *J. Atmos. Sci.* **35** 561–571
- [13] Reynolds W C and Tiederman W G 1967 Stability of turbulent channel flow, with application to Malkus’s theory *J. Fluid Mech.* **27** 253–272
- [14] Farrell B F and Ioannou P J 1996 Generalized stability. Part II: Non-autonomous operators *J. Atmos. Sci.* **53** 2041–2053
- [15] Trefethen L N, Trefethen A E, Reddy S C and Driscoll T A 1993 Hydrodynamic stability without eigenvalues *Science* **261** 578–584
- [16] Gebhardt T and Grossmann S 1994 Chaos transition despite linear stability *Phys. Rev. E* **50** 3705–3711
- [17] Baggett J S and Trefethen L N 1997 Low-dimensional models of subcritical transition to turbulence *Phys. Fluids* **9** 1043–1053
- [18] Grossmann S 2000 The onset of shear flow turbulence *Rev. Mod. Phys.* **72** 3705–3711
- [19] Jiménez J and Pinelli A 1999 The autonomous cycle of near-wall turbulence *J. Fluid Mech.* **389** 335–359

- [20] Hamilton K, Kim J and Waleffe F 1995 Regeneration mechanisms of near-wall turbulence structures *J. Fluid Mech.* **287** 317–348
- [21] Farrell B F and Ioannou P J 2017 Statistical state dynamics-based analysis of the physical mechanisms sustaining and regulating turbulence in Couette flow *Phys. Rev. Fluids* **2** 084608
- [22] Farrell B F and Ioannou P J 1999 Perturbation growth and structure in time dependent flows *J. Atmos. Sci.* **56** 3622–3639
- [23] Wolfe C L and Samelson R M 2007 An efficient method for recovering Lyapunov vectors from singular vectors *Tellus A* **59** 355–366
- [24] Ding X, Chaté H, Cvitanović P, Siminos E and Takeuchi K A 2016 Estimating the dimension of an inertial manifold from unstable periodic orbits *Phys. Rev. Lett.* **117**(2) 024101
- [25] Nikolaidis M A, Farrell B F, Ioannou P J, Gayme D F, Lozano-Durán A and Jiménez J 2016 A POD-based analysis of turbulence in the reduced nonlinear dynamics system. *J. Phys.: Conf. Ser.* **708** 012002